Available online at www.sciencedirect.com
SCIENCE DIRECT®
Journal of Solid State Chemistry 177 (2004) 3119–3126
JOURNAL OF SOLID STATE CHEMISTRY
http://elsevier.com/locate/jssc

Synthesis and characterization of the novel $Nb_3O_5F_5$ niobium oxyfluoride: the term $n = 3$ of the $Nb_nO_{2n-1}F_{n+2}$ series

Stéphane Cordier,[a,*] Thierry Roisnel,[a] and Marcel Poulain[b]

[a] *Laboratoire de Chimie du Solide et Inorganique Moléculaire, UMR 6511 CNRS-Université de Rennes1, Institut de Chimie de Rennes, Avenue du Général Leclerc, 35042 Rennes Cedex, France*

[b] *Laboratoire des Matériaux Photoniques, UMR 6512 CNRS-Université de Rennes1, Institut de Chimie de Rennes, Avenue du Général Leclerc, 35042 Rennes Cedex, France*

Received 19 November 2003; received in revised form 11 May 2004; accepted 12 May 2004

Available online 8 July 2004

Abstract

The solid-state synthesis of the oxyfluoride $Nb_3O_5F_5$, its crystal structure determined from X-ray powder diffraction data as well as some physical characterizations, are reported. $Nb_3O_5F_5$ constitutes the term $n = 3$ of the $Nb_nO_{2n-1}F_{n+2}$ series related to the Dion–Jacobson phases. It crystallizes, at room temperature, in the tetragonal system (space group *I4/mmm* (no. 139); $Z = 4$; $a = 3.9135(1)$ Å, $c = 24.2111(2)$ Å, and $V = 370.80(3)$ Å^3). The crystal structure appears to be an in-between of the three-dimensional network of NbO_2F and the two-dimensional packing of $NbOF_3$ (term $n = 1$ of the $Nb_nO_{2n-1}F_{n+2}$ series). This layered structure consists of slabs made of three $Nb(O,F)_6$ corner-linked octahedra in thickness ($n = 3$) shifted one from another by a $(\frac{1}{2}a + \frac{1}{2}b)$/translation. Oxygen and fluorine atoms are randomly distributed over all the ligand sites.

Keywords: Niobium; Oxyfluoride; Dion–Jacobson phases; X-ray powder diffraction; Layered structure

1. Introduction

Complex fluorides of general formula $A_xM_yF_z$ (A = alkaline element; M = transition element) crystallize in numerous structure types [1], which can be described as various stackings of $(MF_6)^{n-}$ octahedra sharing apices, edges, or faces with adjacent groups. The cohesion as well as the neutrality of the compounds is ensured by additional A cations that fill the vacancies of these architectures. The type of condensation of octahedra depends on the size of the M transition element and its charge. Many compounds in which the direct linking of octahedra occurs along one, two, or three directions (one dimensional (1D), two dimensional (2D), and three dimensional (3D)) have been reported in the literature [1,2].

Among the various structures encountered in fluorides, the topology of the K_2NiF_4 monolayered structure provides the basic model from which are related the structures of several layered oxide families (Aurivilius ($Bi_2O_2[A_{n-1}M_nO_{3n+1}]$) [3], Dion–Jacobson ($A'[A_{n-1}M_nO_{3n+1}]$) [4,5], and Ruddlesden—Popper (R–P) ($A'_2[A_{n-1}M_nO_{3n+1}]$) [6]). Many research works have been devoted to the latter series in the view of their interesting physico-chemical properties such as photo-catalytic behavior [7], brönsted acidity [8], ionic conductivity [9], and intercalation behavior [5].

The stabilization of M_nX_{3n+1} networks without A extra cations should enhance the intercalation properties of such layered materials. One strategy implemented in the present work, in order to obtain M_nX_{3n+1} networks without cations, consists in compensating the loss of the cationic charge by the replacement of oxygen by fluorine. This applies, in particular, to the Dion–Jacobson series in which the transition element is niobium. Furthermore, another attractive feature in the Nb–O–F system is that the geometric arrangement of the $Nb(O,F)_6$ octahedra, and consequently the structural dimensionality, is directly correlated to the (O,F)/Nb ratio. Indeed, the NbO_2F oxyfluoride is usually described as a ReO_3-type (3D network) array

*Corresponding author. Fax: +33-2-99-63-57-04.
E-mail address: stephane.cordier@univ-rennes1.fr (S. Cordier).

0022-4596/$ - see front matter © 2004 Elsevier Inc. All rights reserved.
doi:10.1016/j.jssc.2004.05.032

of $Nb(O,F)_6$ octahedra sharing corners [10,11]. The increase of the (O,F)/Nb ratio must lead to non-bridging anions within the structure to account for the gross of the chemical formula. It will result in the stabilization of layered structures, crystallographically related to that of ReO_3, by a virtual 'shear mechanism'. The ultimate term of this crystallographic 'sharing' has already been obtained for the monolayered $NbOF_3$ oxyfluoride [12], isostructural to NbF_4 [13]. It exhibits a 2D structure based on $Nb(O,F)_6$ octahedra with two terminal anions located in opposite direction and the four other ones, corner-shared with adjacent $Nb(O,F)_6$ octahedra in the equatorial plane.

This simple approach suggests that for a (O,F)/Nb ratio ranging from 3 to 4, homologous Nb_nX_{3n+1} series should be obtained. Their structures should consist in 2D slabs of ReO_3 type whose thickness would decrease as the (O,F)/Nb ratio becomes close to 4. These series could be described as empty *A*-cation-layered perovskites [4,5].

The present work reports the first results of our investigations on anion excess compounds with the general formula $Nb_nO_{2n-1}F_{n+2}$ $(0<n\leqslant 1)$, in which n also measures the thickness of the slabs. The monolayered $NbOF_3$ (2D) and NbO_2F (3D) correspond to the first ($n=1$) and final terms of this series, respectively. The synthesis and the characterization of the novel $Nb_3O_5F_5$ niobium oxyfluoride that constitutes the term $n=3$ are described here.

2. Experimental

2.1. Synthesis

$Nb_3O_5F_5$ was obtained starting from the NbO_2F and NbF_5 precursors. NbO_2F was synthesized in the laboratory according to the following procedure. Niobium oxide was first fired at room atmosphere to eliminate carbon-containing impurities (dust, grease, or polymer traces). In a second step, it was dissolved in aqueous HF, followed by evaporation and drying in platinum or vitreous carbon crucible. Residual amounts of HF and H_2O adsorbed onto NbO_2F crystalline powder were eliminated in a final heating stage at 350°C for 2 h under argon flow. The X-ray powder diffraction pattern and IR absorption spectrum of the resulting white colored NbO_2F did not reveal the presence of any impurity. Note that NbO_2F is grayish colored and that its IR absorption spectrum shows sharp absorption bands around 1385 and 1260 cm^{-1} when niobium oxide is not fired before use.

Niobium pentafluoride was kindly provided by the Institute of High Purity Substances of Nizny Novgorod (Russia). The X-ray powder diffraction pattern of NbF_5, recorded in a airtight and watertight cell on a Philips X'Pert Pro diffractometer equipped with a X'celerator detector (Co$K\alpha$ radiation), did not reveal the presence of any impurity.

NbO_2F (770 mg) and an excess of NbF_5 (395 mg) were weighted, ground, and formed as a pellet in a controlled atmosphere glove box. Then, it was introduced in a niobium container (Plansee) that was subsequently welded under argon and encapsulated in an evacuated silica ampoule. After 1 month of reaction at 240°C, the tube was opened and the excess of NbF_5 was eliminated at 120°C under dynamic vacuum. The final product was obtained as a blue bulk sample stable on air. Contrary to NbF_4 and $NbOF_3$ ($n=1$), $Nb_3O_5F_5$ is easily handled and is stable at room atmosphere. No evolution of the X-ray diffraction pattern has been observed after several weeks. This suggests that the hygroscopicity of the $Nb_nO_{2n-1}F_{n+2}$ series decreases as fluorine content decreases (decrease of n). Further experiments have demonstrated that the same reproducible results can be obtained after 1 week of reaction in nickel containers. The crucial practical problem during the chemical synthesis lies in the strong hygroscopic character of NbF_5. It reacts rapidly with water traces to product NbO_2F according to the chemical reaction: $NbF_5+2H_2O\rightarrow NbO_2F+4HF$. Consequently, in order to limit hydrolysis phenomena that could modify the NbO_2F content in the loaded starting composition, all sampling steps were carried out in a very dry glove box, less than 5 ppm in water.

2.2. Chemical analysis

The O/F ratio was measured by accurate WDS–EPMA (wavelength dispersive X-ray spectrometer–electron probe microanalyzer) measurements using a Camebax SX 50 microprobe, equipped with five spectrometers and a variety of crystals to make accessible the radiation characteristics of the full range of elements (atomic weight greater than He). Bulk samples have been embedded in epoxy resin and polished down to 0.25 mm diamond grade, in order to obtain a perfect plane surface. The measurements were performed on several points of the sample, each of them exhibiting Nb, O, F element. It turned out that the bulk composition was very homogeneous. The experimental average atomic percentage composition determined using all these measurements are the following: Nb: 23.5 (4); O: 38.9 (9); and F: 37.6 (9). These values are in agreement with the $Nb_3O_5F_5$ formula (Nb: 23.1; O: 38.45; and F: 38.45).

2.3. EPR measurements

EPR spectra of polycrystalline sample were obtained using a Bruker EMX 8/2.7 spectrometer (X-band, $\nu=9.5$ GHz) equipped with an Oxford Instruments

cryogenic unit. Previous EPR studies of Nb_3IF_7L–$(Nb^{IV}L_2)_{0.25}$ (L = O,F), oxyhalide that contains magnetic $Nb^{IV}(O,F)_6$ entities [14], have demonstrated the efficiency of such a technique to evidence the presence of magnetic niobium even in small ratio. In the title compound EPR spectra measured between room temperature and liquid nitrogen did not reveal any trace of magnetic niobium. This feature indicates that the composition does not deviate significantly from the $Nb_3O_5F_5$ stoichiometric composition. However, for a $Nb_3O_5F_5$ stoichiometric composition, the title compound should be colorless. The blue color may be the signature of a small range of homogeneity with a $Nb^{V}_{3-x}Nb^{IV}_{x}O_{5-x}F_{5+x}$ formula attributed to a marginal reduction of Nb^{V}–Nb^{IV}.

2.4. IR measurements

Optical transmission was recorded between 4000 and 100 cm^{-1} using a FTIR Brucker Equinox 55 spectrophotometer. Powdered samples were mixed with KBr or a sampling polymer and pressed to form thin pellets. Apart from two water-related bands originating from sampling, a major absorption zone is observed between 400 and 1100 cm^{-1}. Other absorption bands are located between 370 and 200 cm^{-1} and around 150 cm^{-1}. Three maxima are observed at the highest frequencies: 940, 700, and 485 cm^{-1}. However, accurate observation shows that these bands are not symmetric and suggests that the structure of these bands is complex.

2.5. $Nb_3O_5F_5$ structure from X-ray powder diffraction

Further details of the crystal structure investigation can be obtained from the Fachinformationszentrum Karlsruhe, 76344 Eggenstein-Leopoldshafen, Germany, (Fax: (49) 7247-808-666; e-mail: crysdata@fiz.karlsruhe.de) on quoting the depository number CSD-413533.

2.5.1. High-resolution X-ray data collection

X-ray diffraction data of powdered $Nb_3O_5F_5$ were collected with a Siemens D500 powder diffractometer, in a parafocusing Bragg–Brentano geometry, using a monochromatic Cu$K\alpha$1 radiation ($\lambda = 1.5406$ Å) selected by a curved-crystal germanium monochromator [15]. High-resolution data have been recorded in the 15–149.98 (2θ) angular range with a constant step of 0.02° in 2θ and using a variable counting time strategy [16]: 18 s per point until 64.98° (2θ), 36 s up to 104.98°(2θ), and 54 s to the end of the scan. After data collection, stability of X-ray source was checked by recording again diffraction lines at low 2θ angles. Separate scans were merged into a single data set with a mean constant count time per point and corresponding errors were calculated consequently.[1] Angular Bragg positions for X-ray pattern indexing were determined from the automatic peak search and the profile fitting procedures implemented in the WinPLOTR powder diffraction data analysis program [17]. Pattern indexing was carried out with DICVOL91 [18]. Intensities extraction was performed through the profile pattern matching procedure using FULLPROF program [19]. Structure solution was determined by direct method techniques, using EXPO [20]. Finally, Rietveld profile refinements have then been carried out using FULLPROF.

2.5.2. Diffraction pattern indexing

The first 17 diffraction lines of the X-ray pattern were indexed on the basis of tetragonal symmetry with the unit-cell dimensions $a = 3.916(1)$ Å and $c = 24.222(3)$ Å, and the following figures of merit: $M(17) = 58.2$ [21], $M'(17) = 290.8$ [22], and $F(17) = 42.8(0.0065, 61)$ [23]. Starting from this solution, the whole diffraction pattern was indexed and refined: observed extinctions ($h + k + l = 2n \pm 1$) were found to be compatible with a centered unit cell.

2.5.3. Structure determination

On the basis of this centered tetragonal unit cell, the whole diffraction pattern was refined in a profile matching mode with the FULLPROF program, leading to the extraction of 150 integrated intensities. Starting from the more symmetric space group (i.e., $I4/mmm$) and a Z parameter value equal to 2, this set of integrated intensities was used as input data for the solving structure EXPO program, which rapidly revealed positions of niobium and anions.

2.5.4. Structure refinement

Rietveld least-squares refinement was carried out in the whole 2θ angular range (Fig. 1). Due to the very small difference in the X-ray scattering power of oxygen and fluorine (only one electron), first refinements were performed assuming that anionic positions were occupied by a 50% oxygen–50% fluorine mixture.

Attempts to refine the anionic populations have been realized, including restraints on site multiplicities, total stoichiometry, and thermal factors. No significant

[1] n is the number of measured points in the diffraction pattern, t_i is the acquisition time for point i, $\langle t \rangle$ is the mean acquisition time, Y_i is the measured counting for point i (for t_i), nY_i is the normalized counting for point i (for $\langle t \rangle$), $\sigma(nY_i)$ is the sigma of nY_i

$$\langle t \rangle = \frac{1}{n}\sum_{i}^{n} t_i,$$

$$nY_i = \frac{\langle t \rangle}{t_i} Y_i,$$

$$\sigma(nY_i) = \frac{\langle t \rangle}{t_i} \sqrt{Y_i}.$$

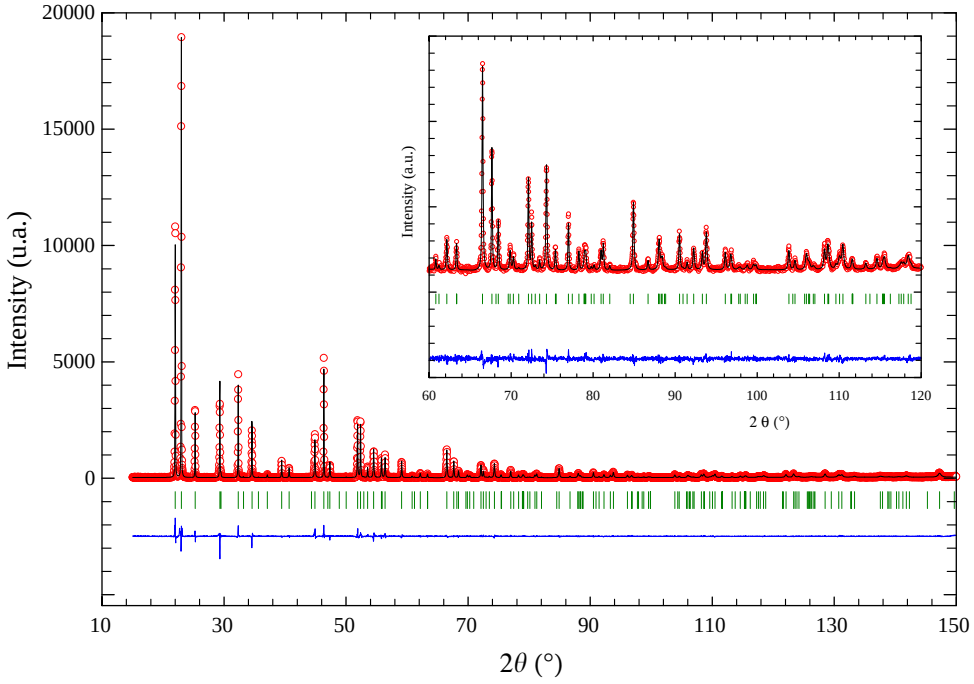

Fig. 1. Observed (dotted line) and calculated (solid line) of the final Rietveld refinement. The lower line is relative to the difference pattern ($Y_{obs}-Y_{calc}$), whereas vertical tics correspond to the 2θ Bragg positions.

Table 1
Rietveld refinement conditions

Diffractometer	D500 Siemens
Wavelength (Å)	1.5406 Å
Sin θ/λ	0.627 Å^{-1}
Number of reflections	149
Number of structural dependent parameters	13
Number of profile dependent parameters	10
Background description	Linear interpolation between 24 refined points
Profile function	Thompson–Cox–Hastings pseudo–Voigt
Agreement factors	
R_p (%)	10.5
R_{wp} (%)	13.6
R_{exp} (%)	10.6
χ^2 (%)	1.65
R_B (%)	4.3
R_F (%)	2.7

improvement of the Rietveld refinement as well as no significant preferential anionic ordering could be evidenced. Owing to the absence of single crystals, no anionic ordering can be clearly evidenced or excluded from powder diffraction data analysis. As stressed in the following discussion, the 50/50 occupation is corroborated by structural consideration—mainly bond lengths—after the analysis of related niobium oxides based on Nb_3O_{10} network.

The details on the Rietveld refinement conditions are listed in Table 1. Crystallographic features and selected atomic distances and angles are summarized in Tables 2 and 3, respectively.

3. Results

3.1. Structural description

$Nb_3O_5F_5$ is the third member of the homologous series $Nb_nO_{2n-1}F_{n+2}$. Indeed, as one could expect, the crystal structure of the $Nb_3O_5F_5$ oxyfluoride appears to be an in-between of the 3D network of NbO_2F and the 2D packing of $NbOF_3$. The structure may be conveniently depicted as the association of one layer of the NbO_2F structure with two layers of the $NbOF_3$ structure (Fig. 2) resulting in a slab of three $Nb(O,F)_6$ octahedra in thickness. For clarity in the following, the $X1$ and $X2$ ligand sites locating within the layer will be called *equatorial*, the $X4$ ligands sites located between layers will be called *median* and the $X3$ ligands will be called *apical* (Fig. 3). Then the general formula can be written $Nb3X_{12/2}^{equa}X_{2/2}^{median}X_{2}^{apical}$. The $Nb2X2_4^{equa}X4_2^{median}$ octahedra belonging to central layers are very regular with almost equal $Nb2-X2^{equa}$ and $Nb2-X4^{median}$ interatomic distances. The $Nb1X1_4^{equa}X4^{median}X3^{apical}$ octahedra belonging to external layer are somewhat distorted along the direction perpendicular to the layer (c-axis).

As previously observed in $NbOF_3$, owing to the absence of counter-cations, the a parameter in $Nb_3O_5F_5$ is twice less than that of the $M^ICa_2Nb_3O_{10}$ [4] Dion–Jacobson series. In the latter, it appears that the

Table 2
Structural parameters from Rietveld refinement

Atom	Wyckoff site	x	y	z	B^*_{equiv} (Å^2)	Occ.
Space group: *I4/mmm* (139): $a = 3.9135(1)$ Å, $c = 24.2111(2)$ Å						
Nb1	4*e*	0	0	0.1638(2)	1.07*	1
Nb2	2*a*	0	0	0	2.08*	1
*X*1	8*h*	1/2	0	0.1589(9)	1.05(13)	50% O + 50% F
*X*2	4*c*	0	1/2	0	1.00(24)	50% O + 50% F
*X*3	4*e*	0	0	0.2390(9)	1.13(13)	50% O + 50% F
*X*4	4*e*	0	0	0.0811(9)	1.01(13)	50% O + 50% F

[Image] except for X1, X2, X3 and X4—refined isotropically—in which case the isotropic displacement parameters are given.

Table 3
Selected interatomic distances (in Å)

$4 \times d$ (Nb1–*X*1) = 1.9603 (5)	$4 \times d$ (Nb2–*X*2) = 1.9568 (1)
$2 \times d$ (Nb1–*X*3) = 1.8225 (70)	$2 \times d$ (Nb2–*X*4) = 1.9640 (73)
$2 \times d$ (Nb1–*X*4) = 2.0010 (74)	

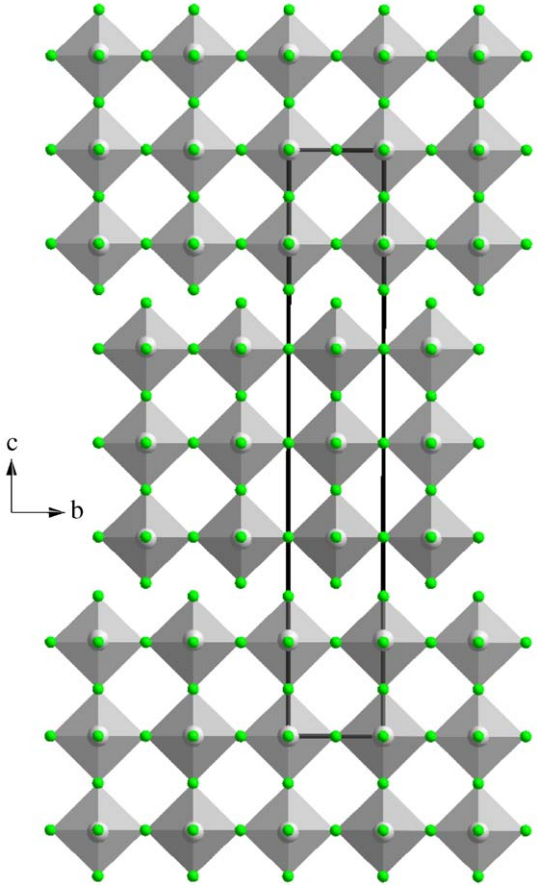

Fig. 2. Representation of the stacking of the Nb_3X_{10} layers along the [100] direction. The unit cell is in bold.

staking of the slabs strongly depends on the size of the *M* counter-cations. With sodium cation the slabs are shifted one from another by a $(\frac{1}{4}a + \frac{1}{4}b)$ translation, for potassium the shift is found to be $b/4$, whilst for rubidium a superposition of layers is observed. It turns

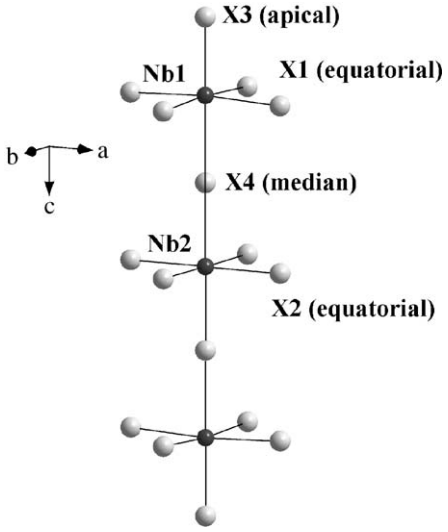

Fig. 3. Representation and labeling of the interconnection of NbX_6 octahedra along the *c*-direction within the Nb_3X_{10} layers.

out that the Nb_3X_{10} network in $Nb_3O_5F_5$—in which a $(\frac{1}{2}a + \frac{1}{2}b)$ shift from one slabs to another is observed—exhibits a topology strongly correlated to the Nb_3O_{10} network in $NaCa_2Nb_3O_{10}$ [4]. Let us point out that the $(\frac{1}{4}a + \frac{1}{4}b)$ shift is observed in the R–P ($A'_2[A_{n-1}M_nO_{3n+1}]$) series whatever the A' interlayer cations. However, since these R–P series are obtained with *M* transition element from different groups (Ti, Mn, Ru…), the use as a prototype of the Dion–Jacobson series is more relevant than the use of the R–P series for the title niobium oxyfluoride because they also involve transition elements from group 5 (Nb or Ta) as *M*. Indeed, in the following, the interatomic distances will be discussed in comparison with Dion–Jacobson layered perovkites containing Nb_3O_{10}, Nb_2O_7, and Nb_2O_6F blocks.

3.2. Vibrational spectroscopy analysis

Vibrational spectroscopy provides additional data from which structural information may be gained. Infrared absorption spectra of niobium oxyfluoride anion and solid compounds have been reported [12,14,24]. They exhibit several bands which have been

interpreted as stretching vibrations (Nb = O (985 cm^{-1}) and Nb–F (595 cm^{-1})), bridging oxygen–niobium vibrations (770 cm^{-1}), and F–Nb–F bridging modes (500 cm^{-1}). In a semi-empirical approach, the IR absorption spectra of NbO_2F, $NbOF_3$, and $Nb_3O_5F_5$ (Fig. 4) have been recorded. The first emerging feature is the similarity between the three spectra that contain three main absorption bands around 500, 700, and 950 cm^{-1}. Note that the IR spectrum of WO_3 also exhibits three bands between 700 and 1000 cm^{-1}. Then, one may conclude that these three bands correspond to different vibration modes of the apex sharing MX_6 octahedra. Indeed, NbO_2F, $NbOF_3$ are built up from one crystallographically independent $Nb(O,F)_6$ octahedron containing 0 and 2 non-bridging anions, respectively, whilst $Nb_3O_5F_5$ is built up from two crystallographically independent $Nb(O,F)_6$ octahedra containing 0 and 1 non-bridging anion. It transpires that the non-bridging anions (either O or F) do not result in new bands, but rather induce some shift in wavelength, related to the change of the vibration energy. On the other hand, $NbOF_3$ and $Nb_3O_5F_5$ spectra appear more complex than that of NbO_2F as illustrated by the 700 cm^{-1} band in the $Nb_3O_5F_5$ spectrum that contains three shoulders. This feature may be explained by different F/O repartition over the ligand sites of the $Nb(O,F)_6$ octahedra. For instance, building $Nb(O,F)_6$ octahedron from NbO_2F requires four oxygen and two fluorine anions. Consequently, two possible configurations can be drawn depending on whether the two fluorine anions are adjacent or not. $NbOF_3$ exhibits a 2D structure based on $Nb(O,F)_6$ octahedra with two terminal anions located in the opposite direction and the four other ones corner-shared with adjacent $Nb(O,F)_6$ octahedra in the equatorial plane. As a result, one $NbOF_5$ octahedron may be constructed with one terminal oxygen, while two different NbO_2F_4 octahedra may exist with equatorial oxygens in the opposite or adjacent locations in the equatorial plane [12].

The IR spectrum of $Nb_3O_5F_5$ appears to be exactly the sum of the NbO_2F and $NbOF_3$ spectra. This analysis corroborates a F/O repartition over all the ligand site in $Nb_3O_5F_5$.

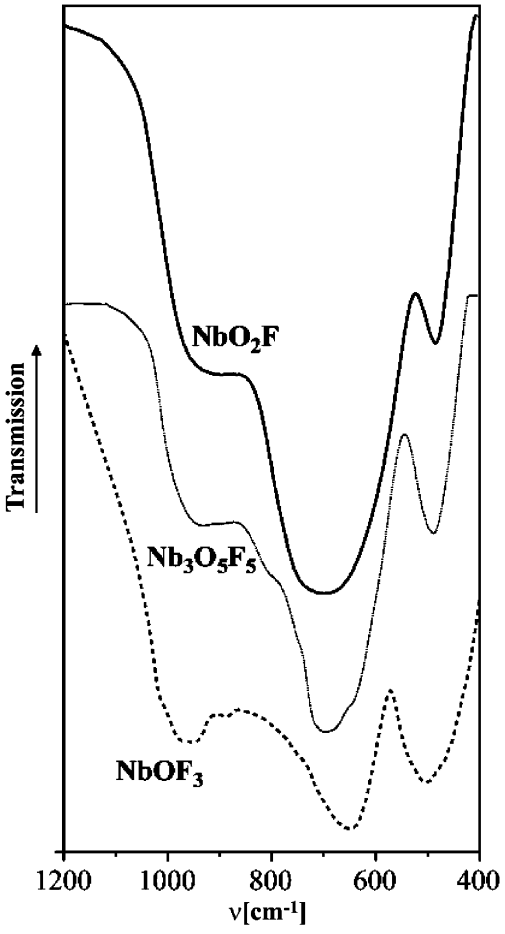

Fig. 4. Infrared spectrum of NbO_2F, $NbOF_3$, and $Nb_3O_5F_5$.

4. Discussion

The analysis of the bond lengths in layered perovskite based on Nb_3O_{10} slabs as, for instance, $Ag_2[Ca_{1.5}Nb_3O_{10}]$ [25] evidences an almost regular NbO_6 octahedron constituting the central layer ($Nb–O^{median}$: 1.977(16) Å × 2; $Nb–O^{equatorial}$: 1.950(1) Å). On the other hand, the NbO_6 octahedron from the external layer is distorted in the direction perpendicular to the layer ($Nb–O^{equatorial}$: 1.962(1); $Nb–O^{median}$: 2.141(16); $Nb–O^{apical}$: 1.849(17)). The discrepancy between the $Nb–O^{median}$ and the $Nb–O^{apical}$ bond length is explained by the $Nb=O^{apical}$ double bond compared to the $Nb–O^{median}$ simple bond. Such discrepancy between the $Nb–O^{median}$ and the $Nb–O^{apical}$ can be observed in all other layered perovskites based on Nb_3O_{10} network such as $Li_4Sr_3Nb_6O_{20}$ [26], as well as in compounds based on Nb_2O_7 double layers such as $Rb_2LaNb_2O_7$ [27].

This systematic distortion observed in oxides evidences that the shorter $Nb1–X^{apical}$ bond length compared to the $Nb2–X^{median}$ one observed in $Nb_3O_5F_5$ must not be attributed to different O/F ratio on the X^{apical} and X^{median} sites. On the contrary, the quite regular geometry of the $Nb1X_6$ octahedron from the central layer with close $Nb1-X1^{equatorial}$ and $Nb2-X2^{equatorial}$ distances suggest that the O/F ratio is very close to 50/50 on $X1^{equatorial}X2^{equatorial}$ and X^{median}. Consequently, owing to the site multiplicities and to the $Nb_3O_5F_5$ stoichiometry the O/F ratio on the X^{apical} site must also be 50/50. In other words, the observed bond lengths agree with a 50/50 fluorine/oxygen distribution on all the ligand sites. The 50/50 repartition of fluorine and oxygen atoms on all ligand sites is corroborated by bond valence method calculation [28a] (included in last

version of FULLPROF program that use R_0 value from Ref. [28b] performed after the last cycle of refinements for Nb_1 and Nb_2 (Nb_1: 5.30(2) and Nb_2: 5.08(2)). These values slightly change when taking R_0 value from Ref. [28c] (Nb_1: 5.06(2) and Nb_2: 4.80(2)).

The Nb1–X^{apical} distance is close to that found in $NbOF_3$ [12] and lies between the Nb=O and Nb–F bond lengths in related oxyfluorides and fluorides. The average Nb–$X^{equatorial}$ values (1.958 Å) are lower than those observed in $NbOF_3$ (1.984 Å), which may be explained by a higher O/F ratio. The Nb–O^{apical} bond length in $ASrNb_2O_6F$ [29], for which the X^{apical} site is not affected by fluorine occupation, and Na_3NbOF_6 [30] are 1.74(2) and 1.738 Å, respectively, and correspond to Nb=O double bonds. In the ordered oxyfluoride $NaNbO_2F_2$ [31], the Nb–F terminal distances are found to be 1.995 and 2.038 Å, whilst they are 1.887 Å in NH_4NbOF_4 Å [32].

The average structure obtained by X-ray powder diffraction for $Nb_3O_5F_5$ leaves open the question whether some local fluorine and oxygen ordering occurs around niobium. Indeed, the recent investigation of the $NbOF_2$ structure [33] has clearly demonstrated a local ordering of fluorine and oxygen ligands on ligand sites. It turns out that locally the $Nb(O,F)_6$ octahedron is submitted to dynamically excited rigid unit mode (RUM) rotations. Indeed, the Nb–(O,F) distance (1.951 Å) in NbO_2F that is obtained from structural refinement of XRD data corresponds to the average position of the anions. Locally O or F are shifted from this average position within the $Nb(O,F)_6$ octahedron leading to Nb–O and Nb–F distances of 1.908 and 2.127 Å, respectively [33]. The Nb–X distances in the $Nb_3O_5F_5$ structure lie between the latter distances. The local discrepancy of the Nb–F and Nb–O interatomic distances and the local ordering of oxygen and fluorine is likely to lead to puckered sheets within the slabs. This puckering is not observed for NbO_2F and $NbOF_3$ from X-ray diffraction analysis. It is interesting to note that in $Nb_3O_5F_5$, the $X2-Nb2-X2$ angle is 180°, whereas the $X1-Nb1-1$ angle is 175° in accordance with the conclusion drawn about the puckered sheets in NbO_2F and $NbOF_3$ [12,33].

5. Concluding remark

The solid-state synthesis of the $Nb_3O_5F_5$ oxyfluoride has been reported in this work. The crystal structure determined by X-ray powder diffraction appears to be an in-between of the 3D network of NbO_2F and the 2D packing of $NbOF_3$. $Nb_3O_5F_5$ constitutes the term $n = 3$ of $Nb_nO_{2n-1}F_{n+2}$ series directly related to $M^ICa_2Nb_3O_{10}$ Dion–Jacobson series and, in particular, to the $NaCa_2Nb_3O_{10}$ oxide. The $Nb_3O_5F_5$ compound shows a great deal of interest knowing that Nb^V is easily reduced to Nb^{IV} and that its lacunar character make it ideal host for insertion or intercalation of light elements. Intercalation studies of this new material are now in progress.

Acknowledgments

The authors are very grateful to T. Bataille (LCSIM UMR CNRS 6511, Rennes) for his contribution to the X-ray powder diffraction measurements on $Nb_3O_5F_5$ compound as well as P. Gravereau and S. Pechev (ICMCB-CNRS, Pessac) for measurement of NbF_5 hygroscopic diffraction data. M. Bohn (IFREMER, Brest) is greatly acknowledged for his assistance in EPMA studies as well as C. Perrin (LCSIM UMR CNRS 6511, Rennes) for helpful discussions. We are also indebted to J.-Y. Thépot for EPR studies (LCSIM UMR CNRS 6509, Rennes). We are grateful to "Fondation Langlois" for its financial support.

References

[1] D. Babel, A. Tressaud, in: P. Hagenmuller (Ed.), Material Science Series, Inorganic Solid Fluorides, Academic Press, New York, 1985, p. 77.
[2] G. Ferey, in: R. Bruce King, (Ed.), Encyclopedia of Inorganic Chemistry, Vol. 3, Wiley, New York, 1995, p. 1218.
[3] (a) B. Aurivillius, Ark. Kemi. 1 (1949) 463–499;
(b) B. Aurivillius, Ark. Kemi. 2 (1950) 519.
[4] M. Dion, M. Gane, M. Tournoux, Mater. Res. Bull. 16 (1981) 1429.
[5] A.J. Jacobson, J.W. Johnson, J.T. Lewandowski, Inorg. Chem. 24 (1985) 3727.
[6] (a) S.N. Ruddlesden, P. Popper, Acta Crystallogr. 10 (1957) 538;
(b) S.N. Ruddlesden, P. Popper, Acta Crystallogr. 11 (1958) 54.
[7] J. Yoshimura, Y. Ebina, J. Kondo, K. Domen, A. Tanaka, J. Phys Chem. 97 (1993) 1970.
[8] J. Gopalakrishnan, S. Uma, V. Bat, Chem. Mater. 5 (1993) 132.
[9] S.H. Byeon, K.J. Park, M. Itoh, J. Solid State Chem. 121 (1996) 430.
[10] L.K. Frevel, H.W. Rinn, Acta Crystallogr. 9 (1956) 626.
[11] A.W. Sleight, Inorg. Chem. 8 (1969) 1764.
[12] J. Köhler, A. Simon, L. van Wüllen, S. Cordier, T. Roisnel, M. Poulain, M. Somer, Z. Anorg. Allg. Chem. 628 (2002) 2683.
[13] (a) H. Schäfer, H.G.v. Schnering, K.J. Niehus, H.G. Nieder-Varhrenholz, J. Less-Common Met. 9 (1965) 95;
(b) F.P. Gortsema, R. Didchenko, Inorg. Chem. 4 (1965) 182.
[14] S. Cordier, O. Hernandez, J.Y. Thépot, A.I. Shames, C. Perrin, Inorg. Chem. 42 (2003) 1101.
[15] D. Louër, J.L. Langford, J. Appl. Crystallogr. 21 (1988) 430.
[16] J.K. Cockroft, Commission on Powder Diffraction, Newsletter 27 (2002) 23.
[17] T. Roisnel, J. Rodríguez-Carvajal, Materials Science Forum, In: R. Delhez, E.J. Mittemeijer (Eds.), Proceedings of the Seventh European Powder Diffraction Conference, 2000, p. 118–127.
[18] A. Boultif, D. Louër, J. Appl. Crystallogr. 24 (1991) 987.
[19] J. Rodriguez-Carvajal, Abstracts of the Satellite Meeting on Powder Diffraction of the XV Congress of the IUCr, Toulouse, France, 1990, p. 127.
[20] C. Giacovazzo, D. Siliqi, B. Carrozzini, A. Guagliardi, A.G.G. Moliterni, J. Appl. Crystallogr. 32 (1999) 339.

[21] P.M. De Wolff, J. Appl. Crystallogr. 5 (1968) 108.
[22] A. Altomare, C. Giacovazzo, A. Guagliardi, A.G.G. Moliterni, R. Rizzi, P.E. Werner, J. Appl. Crystallogr. 33 (2000) 1180.
[23] G.S. Smith, R.L. Snyder, J. Appl. Crystallogr. 12 (1979) 60.
[24] J.H. von Barner, E. Christensen, N.J. Bjerrum, B. Gilbert, Inorg. Chem. 30 (1991) 561.
[25] S.P. Bhuvanesh, P.M. Woodward, J. Am. Chem. Soc. 124 (2002) 14294.
[26] N.S.P. Buvanesh, M.P. Crosnier Lopez, O. Bohnke, J. Emery, J.L. Fourquet, Chem. Mater. 11 (1999) 634.
[27] A.R. Armstrong, P.A. Anderson, Inorg. Chem. 33 (1994) 4366.
[28] (a) I.D. Brown, D. Altermatt, Acta Crystallogr. B 41 (1985) 244;
(b) N.E. Brese, M. O'Keeffe, Acta Crystallogr. B 47 (1991) 192;
(c) M. O'Keffee, N.E. Brese, J. Am. Chem. Soc. 113 (1991) 3225.
[29] J.H. Choy, J.Y. Kim, S.-J. Kim, J.S. Sohn, O.H. Han, Chem. Mater. 13 (2001) 906.
[30] R. Stomberg, Acta Chem. Scand. 38 (1984) 603.
[31] S. Anderson, J. Galy, Acta Crystallogr. B. 25 (1969) 847.
[32] V.I. Pakhomov, T.A. Kaidalova, Kristallografiya 19 (1974) 733.
[33] F.J. Brink, R.L. Withers, L. Norén, J. Solid State Chem. 166 (2002) 73.